On-nanowire spatial bandgap design for white light emission

Zongyin Yang,[†] Jinyou Xu,[‡] Pan Wang,[†] Xiujuan Zhuang,[‡] Anlian Pan,[‡,*] and Limin Tong[†,*]

[‡]College of Physics and Microelectronics Science, Key Laboratory for Micro-Nano Physics and Technology of Hunan Province, Hunan University, Changsha 410082, China
†State Key Laboratory of Modern Optical Instrumentation, Department of Optical Engineering, Zhejiang University, Hangzhou 310027, China
*Email: Anlian.pan@hnu.edu.cn; phytong@zju.edu.cn

Introduction

Color controlled solid-state light emitting, especially semiconductor-based solid-state white lighting, has attracted great attention for the higher conversion efficiency and more flexible control of photometric properties compared with the conventional incandescent lighting.[1] White light can be formed by mixing lights of differently colors, such as red, green, and blue (RGB). A feasible approach is to mix light emitting diodes (LEDs) of the proper wavelengths and intensity ratios.[2] Although this route has the potential for high luminous efficiency,[3] low color rendering index (CRI) and stability make it little aesthetically pleasing. The other approach is to combine the phosphor-based wavelength down-conversion medium with a blue or UV light excitation.[4] Though this phosphor-based white technology can achieve a good color quality, its efficiency is severely limited by the inevitable Stokes energy loss which is not incurred in the semiconductor-based white light sources. A major challenge in solid-state lighting research is to achieve rationally designed semiconductor-based light-emitting materials or structures with both reasonable power efficiency and color quality.[5]

The well-developed nanotechnology brings new opportunities for solid-state white lighting researches.[6,7,8·····16] In particular, semiconductor nanostructures, such as semiconductor alloy nanowires, have shown the potential in constructing white lighting sources for their high quantum efficiency and wide bandgap tunability.[17, 18, 19] Using the vapor-liquid-solid (VLS) nanowire growth mechanism, the element composition in the grown nanowires can directly be controlled by the corresponding element concentration in the source materials or the precursor vapor,[20, 21, 22, 23, 24, 25] and semiconductor alloys with different bandgaps can be gradually grown into single wires along their length, through applying an *in situ* concentration changing of the source reagents during the

growth.[6, 26, 27……33] These bandgap graded semiconductor nanostructures take the chances to design novel white light-emitting materials or structures at microscale from the ground up.

To realize white light-emitting of bandgap graded semiconductor nanowires, the most important issue is to get wires with bandgap tunability in the entire visible region, and have the capability to selectly control the bandgap/composition along the wires. Due to the differences in condensation temperatures and growth kinetics during the catalyst-assistant VLS growth, it is observed that alloy nanowires with different alloy compositions could deposit at different positions along the length of the growth tube where a temperature gradient exists.[34, 35] Using this temperature-selected composition dispersive phenomenon, quarternary ZnCdSSe alloy nanowires with bandgap tunability covering the full visible range were grown along the length of a single substrate.[36, 37] In this work, based on this temperature-selected composition dispersion, we developed a substrate moving strategy in the VLS process and realized the growth of composition gradient ZnCdSSe alloy nanowires (full-color nanowires), with gradually tunable bandgaps covering the entire visible range along the length of the wires. More importantly, the relative length of selected bandgap/composition segments along the wires can be controlled during the growth. Using tri-color (RGB) based white emission principle [ ] and through careful composition control, we realized the color-controlled on-nanowire white light emission (tri-color nanowires). This impressive result opens a gate to design nanoscale white light sources, which will find many applications in all kinds of areas.

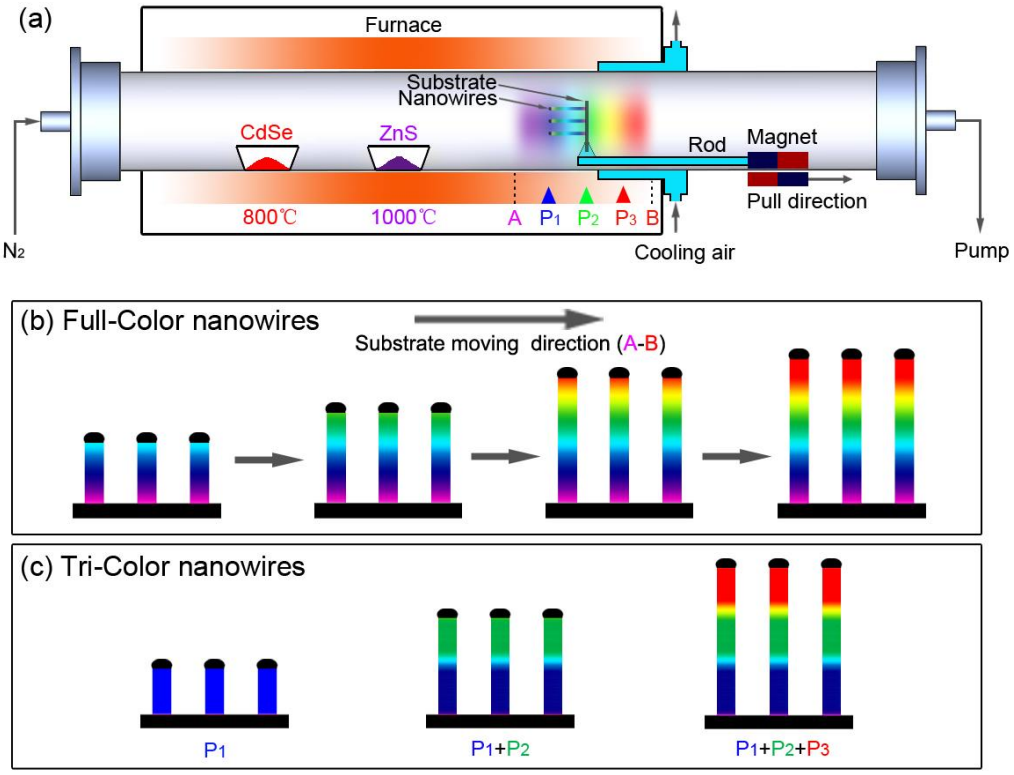

Figure 1. Schematic diagrams of the experimental setup (a) and the growth processes for full-composition (b) and tri-color (c) bandgap graded ZnCdSSe nanowires, respectively.

Figure 1a shows the schematic setup for the growth of full-color bandgap graded ZnCdSSe alloy nanowires. A horizontal quartz tube (inner diameter 45 mm, length 120 cm) was mounted inside a single-zone furnace. In the tube, an alumina boat with ZnS powder (Alfa Aesar, 99.99% purity) was loaded at the center of the heating zone, and the other boat with CdSe powder (Alfa Aesar, 99.995% purity) was placed upstream of the tube with a temperature approximate to 800 ℃. A silicon substrate coated with a 2-nm thick gold film was vertically mounted to a quartz rod which was driven by a magnet system during the growth. The different colors of the deposition zone (from positions A to B) at the downstream of the tube indicate the different bandgaps/compositions of the corresponding deposited materials (see Figure 1a). The system was flushed with high-purity N_2 for 1 h to eliminate O_2, and the silicon substrate was located at position A before heating. Then the furnace was rapidly heated to 1000 ℃with a constant flow of 50 SCCM nitrogen gas under a ~15 Torr pressure. Ten minutes later, the silicon substrate was pulled from Position A to Position B by a magnet at the velocity of 5 cm per minute. After 4 minutes' growth in the position B, the furnace was turn off and cooled down to

room temperature naturally. Bandgap graded full-color ZnCdSSe alloy nanowires were collected on the silicon substrate. The formation process of these full-color wires is schematically shown in Figure 1b.

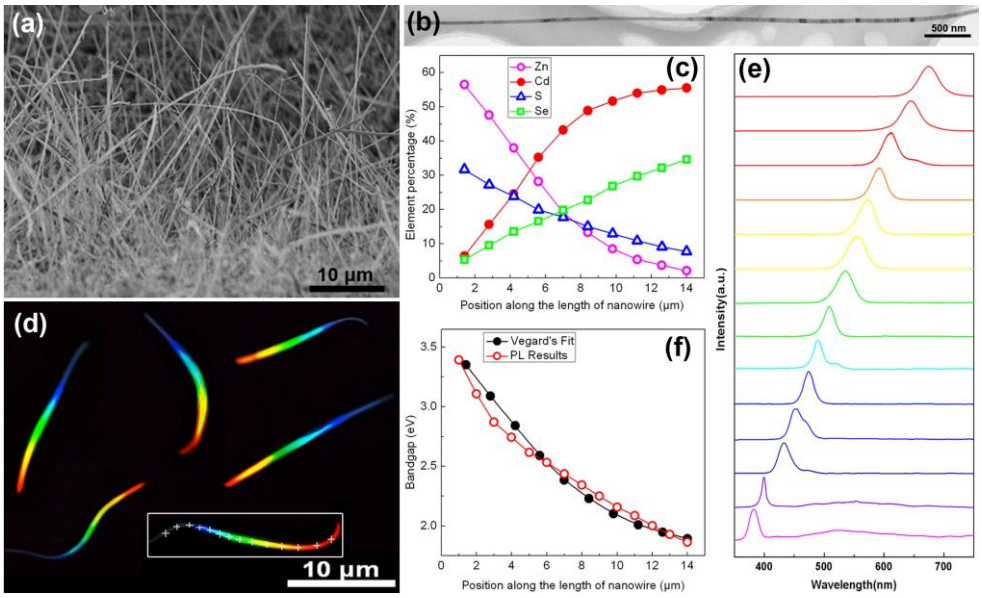

Figure 2. (a) Side-view SEM image of the as-grown sample of full-composition ZnCdSSe nanowires, (b) TEM image of a representative single full-composition wire from the sample, (c) position-dependent element percentages along the length of the wire for elements Zn, Cd, S and Se, respectively, (d) the real-color CCD photograph of several dispersed full-composition ZnCdSSe nanowires under a blend of darkfield and 355 nm laser illuminations, (e) and (f) position-dependent PL spectra (normalized) and bandgap values along the length of a single full-composition wire which is indicated by a white rectangle box in Fig. 3d (see the cross marks for the examined points).

The morphology of the as-grown bandgap graded full-color nanowires was characterized by scanning electron microscope (SEM) and transmission electron microscopy (TEM), as shown in Figures 2a and b, respectively, which indicate that these graded wires have a uniform diameter of ~80 nm and a length from several microns to ~30 μm. The EDX analysis of a representative single wire indicates that any detected points along the length are composed of Zn, Cd, S and Se elements. From the position-dependent element percentages shown in Figure 2c, the element contents of Cd and Se increase gradually from the detected positions along the wire, while the element contents of Zn and S are complementary to those of Cd and Se. High-resolution TEM (HRTEM) and corresponding selected area electron diffraction (SAED) investigations further demonstrate that the obtained wires are highly crystallized along their whole lengths (see the supporting information). The above results confirm the formation of these composition gra-

dient ZnCdSSe alloy nanowires.

The PL properties of these composition gradient nanowires were characterized by a dark-field fluorescence microscopy (Axio Imager Z2m, Carl Zeiss) and a point scanning spectrometer (Mapping, HORIBA Jobin Yvon LabRam HR 800). Some ZnCdSSe wires were removed from the as-grown sample and dispersed on a MgF_2 substrate before measurements. Figure 2d gives the real-color CCD photograph of several dispersed wires under a blend of darkfield and 355 nm laser illuminations, which shows the emission colors of all these nanowires gradually changed along their lengths. The red end corresponds to the Cd/Se-rich alloys, and the other grey end corresponds to the Zn/S-rich alloys with the bandgap or light emission extended into the near ultraviolet (UV) region. The position-dependent photoluminescence (PL) spectra collected along the length of a selected single wire (see the white cross indicted spots in the rectangle box marked wire in Figure 2d) show that every point region has a single-band PL emission, with their peak wavelength gradually changed from ~380 nm to ~700 nm (see Figure 2e), covering the full visible spectrum range. The local bandgap values directly obtained from the PL spectra have good consistency with those calculated from the EDS results combined with the Vegard's law for quarternary ZnCdSSe alloys,[38] indicating all of the observed PLs are from the band-edge emission of the bandgap graded alloys. The above results demonstrate that full-color bandgap graded ZnCdSSe alloy nanowires were achieved by the position/temperature-selected growth which is realized through the moving of the substrate at a constant speed from high temperature to low temperature along the deposition zone.

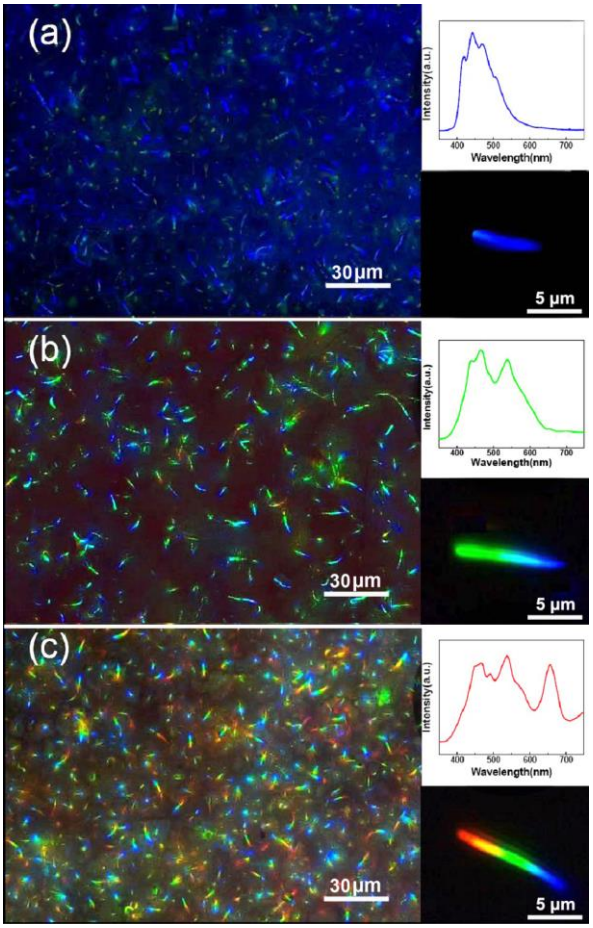

Figure 3. (a)-(c) Top-view real-color PL photographs of the as-grown single-color (a), double-color (b) and tri-color (c) nanowires, respectively. Upper-right insets in each picture, the corresponding in-situ collected PL spectrum; Lower right-insets in each picture, the enlarged photographs of individual wires.

Based on the above growth strategy for full-color bandgap graded ZnCdSSe nanowires, selected composition control along the wires have been conducted by selectively controlling the positions and moving speed of the substrate during the growth. When the substrate is at a fixed position, without any moving during the growth, the obtained nanowires are not composition gradient, having a corresponding position/temperature related constant composition along their whole length. Figure 3a is the real-color picture of the single-color sample grown by keeping the substrate in fixed position P_1, which shows that the grown wires give almost pure blue light under the UV illumination. No apparent color change was observed along the length from the enlarged individual wires (see the lower-right inset in Figure 3a), indicating the grown nanowires are not composition gradient. The *in situ* PL spectrum of the sample (see the upper-right inset of Figure 3a) gives a single emission band with the peak wavelength centered at 475 nm, which is

consistent with the exhibited blue color of the sample. It is reasonable since position P_1 is Zn/S rich, making the grown wires have a wide bandgap. If the substrate firstly stays some time for growth at position P_1, and then moved quickly to another position P_2 where alloys with a narrower bandgap at the "green" region can be deposited for the next growth. The obtained nanowires should have two main composition distributions and thus have double PL emission bands. Figure 3b is the real-color picture of the sample grown using this idea, which shows two main colors (blue and green) along their length. The picture of an enlarged individual wire as well as the *in situ* PL spectrum of the sample further confirm the double-color emission of the wires. Following the same strategy, tri-color nanowires were achieved by changing three positions of the substrate during the growth, i.e. the substrate stays some time in turn at position P_1, P_2 and P_3, for the growth of blue, green and red compositions, respectively. The PL pictures and the corresponding *in situ* spectra of the achieved tri-color wires are shown in Figure 3c and its insets. As expected, the wires have three main color segments along their length, and the PL spectrum contains three emission bands, corresponding to the blue, green and red segments, respectively. The above results demonstrate that selected composition control along individual wires is feasible through this position/temperature-selected growth strategy. Figure 1c shows schematically the different stages of the growth for the composition-selected tri-color wires.

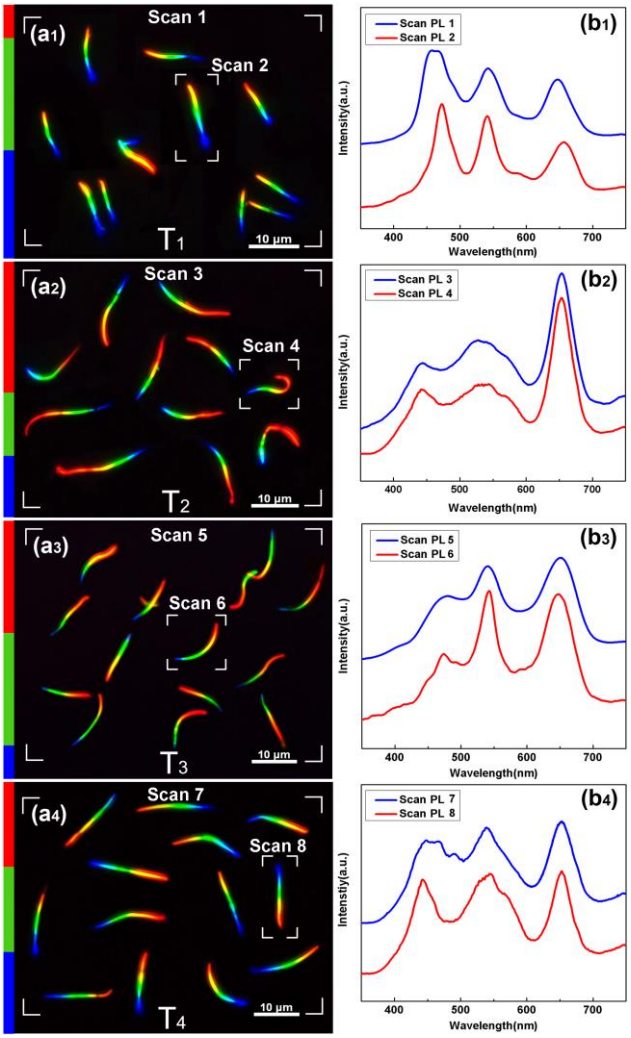

Figure 4. (a_1)-(a_4) The real-color paragraphs of some dispersed nanowires under a 355-nm laser illumination removed from four representative tri-color samples (samples T_1-T_4), respectively. (b_1)-(b_4) the corresponding PL spectra for both the nanowire assembles (blue curve) and the selected single wire (red curve) of the four samples, respectively. The examined nanowire assembles or single wires for PL spectra are indicated in (a_1)-(a_4), respectively. PL collected using DuoScan function of HORIBA Jobin Yvon LabRam HR 800.

The ability of realizing selected composition control along the length and especially the growth of tri-color nanowires prove the potential of achieving "white" light nanowires. To achieve nanowires with ideal white light emission, the relative intensity of the emission bands need be well controlled.[2] Since the intensity of the emission bands are decided by the relative length of the corresponding color segments in the wires, the photometric properties of these tri-color nanowires can be directly controlled by the respective growth time of these segments. Figures 4a_1-a_4 show the real-color paragraphs of some dispersed nanowires under a UV laser illumination removed from four representative tri-color samples (samples T_1-T_4), respectively (see Table S1 in the supporting in-

formation for the respective growing parameters). The wires in sample T_1 have relatively long blue color segments and short red ones, while the red segments in sample T_2 are extremely long compared to the other two kinds of segments. In sample T_3, the blue color segments are very short compared to the others. Sample T_4 is the one which contains wires with comparative length of these three segments. The PL from the nanowire assembles or from a selected wire can both be scanned and collected. Figures b_1-b_4 show the collected PL spectra for both the nanowire assembles (blue curve) and the selected single wire (red curve) of the four samples, respectively. All the spectra compose of three separate emission bands, with their peak positions having very good correspondences to the blue, green and red segments in the wires of each sample, respectively. The differences in the relative intensity of these three emission bands are also in good agreements with the differences of the relative length of color segments in these samples. More important, the spectra of the nanowire assembles are very consistent to the selected single wires in all the examined samples, indicating the composition distribution in all the wires of each sample is highly uniform.

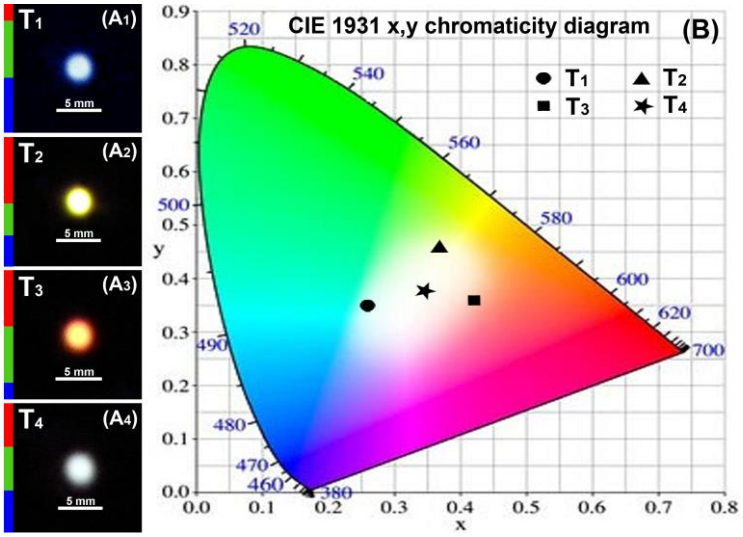

Figure 5. (A_1)-(A_4) the large area real-color paragraphs of the four representative samples (samples T_1-T_4) under the illumination of a beam of UV light, respectively. (B) The CIE chromaticity diagram with the chromatic coordinates and correlated color temperatures of the four representative tri-color samples calculated using the detected PL spectra shown in Figures $4b_1$-b_4, respectively.

The PL photometric properties of these tri-color ZnCdSSe alloy nanowires have been comparatively examined. Figures $5A_1$-A_4 show the large area paragraphs of the dispersed tri-color nanowires under laser illumination removed from four representative

tri-color samples (samples T_1-T_4), respectively. The results show that the PL emissions from samples T_1-T_3 are light blue, light yellow and orange, respectively, while sample T_4 can give a pure white PL emission. The CIE (International Commission on Illumination) chromatic coordinates were calculated using the detected PL spectra shown in Figures $4b_1$-b_4. As shown in Figure 5B, the chromaticity coordinates of samples T_1-T_3 are located at the edge of the white area in the CIE diagram, while that of sample T_4 is located at the center of the white area. The results confirm that only sample T_4 can give pure white light, which is in good agreements with the observations of the real-color PL photographs (Figures $5A_1$-A_4). Different from white lighting using mixed monochrome LEDs, the white light spectra of these tri-color ZnCdSSe alloy nanowires resulted from blending the main three colors and the emissions from the transition regions between these three colors are throughout the entire visible region. Based on the CRI, the broadband spectra white light of tri-color nanowires have higher color quality than narrowband white light spectra of mixed LEDs. Moreover, compare with LEDs array, spatially color mixing of tri-color nanowires would be more uniform due to that all the nanowires act as individual nano/microscale white light sources (see Figure S1 in the supporting information). At the same time, the semiconductor-based tri-color nanowire white lighting also have improved conversion efficiency compared to the conventional phosphor-down-conversion white lighting technology.

As for the growth of tri-color nanowires, except these main experimental parameters shown in Table S1 (see supporting information), some other growth factors should also be taken into account, such as chemical conversion reaction between ZnS and CdSe,[39] thermal conductivity between the substrate and tube, working temperature of CdSe source. When the red segment start growing, the pre-grown blue segment are exposed in CdSe vapour (P_3) and easily converted into red one by ion exchange reaction at the increasing CdSe vapour. Reducing the stay time at P_3 is an effective way to avoid this ion exchange reaction. The poor thermal conductivity between substrate and tube leads to imprecise control of substrate's temperature when it is moving, which will results in the untunable PL photometric properties of nanowires. The strategy in this experiment is to cool tube with a flow of air and fill the gap between substrate and tube with high thermal conductivity material. Low working temperature of CdSe source causes dilute CdSe vapor at P3 which is not suitable for growth of red segment, however, too high CdSe va-

por concentration accelerates the chemical conversion reaction between ZnS and CdSe. In terms of working temperature of CdSe source, 800 ℃is the optimal value.

In summary, using temperature-selected composition deposition realized via a substrate moving assistant CVD route, quarternary ZnCdSSe alloy nanowires, with graded band gap covering the entire visible range along their length, were achieved. At the same time, this growth strategy shows the capability to realize composition selected control by changing the position and moving speed of the substrate during the growth. As a representative, tri-color alloy nanowires have been achieved and the photometric properties of these tri-color nanowires can be controlled by the adjusting the relative lengths of the color segments through carefully modified growth conditions. On-nanowire white light emission has been achieved by the optimized growth. These color-engineered semiconductor alloy nanostructures will have potential applications in multicolor display, multicolor lasers,[40] white lighting, biotechnology and superbroad spectral detectors.

Acknowledgment. The authors thank Dr. Jing Shen and Dr. Suo Ding (HORIBA Jobin Yvon, China) for DuoScan and Mapping characterization of nanowires, Dr. Hua Dai (Carl Zeiss, China) for extended focus photograph, Dr.Yu Ye and Prof. Lun Dai (Peking University) for part of spectral measurement.

Reference

[1] Schubert, E. F.; Kim, J. K. *Science* **2005**, 308, 1274.
[2] Mirhosseini, R; Schubert, M. F.; Chhajed, S.; Cho, J.; Kim, J. K.; Schubert, E. F. *Opt. Exp.* **2009**, 17, 10807.
[3] Zukauskas, A.; Vaicekauskas, R.; Ivanauskas, F; Gaska, R.; Shur, M. S. *Appl. Phys. Lett.* **2002**, 80, 234.
[4] Nakamura, S.; Pearton, D.; Fasol, G. *The Blue Laser Diode: the complete story*, 2nd ed.; Springer 2000.
[5] *Basic Research Needs for Solid-State Lighting*, Report of the Basic Energy Sciences Workshop on Solid-state Lighting, May 22-24, 2006.
[6] Guo, W.; Zhang, M.; Banerjee, A.; Bhattacharya, P. *Nano Lett.* **2010,** 10, 3355.
[7] Yan, R. X.; Gargas, D.; Yang, P. D. *Nat. Photonics* **2009,** 3, 569.
[8] Huang, Y.; Duan, X.; Lieber, C. M. *Small* **2005,** 1, 142.
[9] Gudiksen, M. S.; Lieber, C. M. *J. Am. Chem. Soc.* **2000,** 122, 8801.

[10] Qian, F.; Gradečak, S.; Li, Y.; Wen, C. Y.; Lieber, C. M. *Nano Lett.* **2005,** 5, 2287.
[11] Qian, F.; Li, Y.; Gradecak, S.; Wang, D. L.; Barrelet, C. J.; Lieber, C. M. *Nano Lett.* **2004,** 4, 1975.
[12] Tong, L. M.; Gattass, R. R.; Ashcom, J. B.; He, S. L.; Lou, J. Y.; Shen, M. Y.; Maxwell, I.; Mazur, E. *Nature* **2003,** 426, 816.
[13] Tong, L. M.; Lou, J. Y.; Gattass, R. R.; He, S. L.; Chen, X. W.; Liu, L.; Mazur, E. *Nano Lett.* **2005,** 5, 259.
[14] Gu, F. X.; Yu, H. K.; Wang, P.; Yang, Z. Y.; Tong, L. M. *ACS Nano* **2010,** 4, 5332.
[15] Morales, A. M.; Lieber, C. M. *Science* **1998,** 279, 208.
[16] Zhang, X, M.; Lu, M, Y.; Zhang, Y.; Chen, L.J.; Wang, Z. L. *Adv. Mater.* **2009,** 21, 2767.
[17] Seo, K.; Lim, T.; Kim, S.; Park, H.L.; Ju, S. Nanotechnology **2010,** 21, 255201.
[18] Nguyen, H. P. T.; Zhang, S.; Cui, K.; Han, X.; Fathololoumi, S.; Couillard, M.; Botton, G. A.; Mi, Z. *Nano Lett.* **2011**, 11, 1919.
[19] Lin, H. W.; Lu, Y. J.; Chen, H. Y.; Lee, H. M.; Gwo, S. *Appl. Phys. Lett.* **2010,** 97, 073101.
[20] Pan, A. L.; Yang, H.; Liu, R. B.; Yu, R. C.; Zou, B. S.; Wang, Z. L. *J. Am. Chem. Soc.* **2005,** 127, 15692.
[21] Pan, A. L.; Liu, R. B.; Sun, M. H.; Ning, C. Z. *J. Am. Chem. Soc.* **2009,** 131, 9502.
[22] Pan, A. L.; Wang, X.; He, P.; Zhang, Q.; Wan, Q.; Zacharias, M.; Zhu, X.; Zou, B. S. *Nano Lett.* **2007,** 7, 2970.
[23] Qian, F.; Li, Y.; Gradecak, S.; Park, H.; Dong, Y.; Ding, Y.; Wang, Z. L.; Lieber, C. M. *Nat. Mater.* **2008,** 7, 701.
[24] Persson, A. I.; Bjork, M. T.; Jeppesen, S.; Wagner, J. B.; Wallenberg, L. R.; Samuelson, L. *Nano Lett.* **2006,** 6, 403.
[25] Tian, B. Z.; Kempa, T. J.; Lieber, C. M. *Chem. Soc. Rev.* **2009,** 38, 16.
[26] Gu, F. X.; Yang, Z. Y.; Yu, H. K.; Wang, P.; Tong, L. M.; Pan, A. L. *J. Am. Chem. Soc.* **2011,** 133, 2037.
[27] Yang, J. E.; Park, W. H.; Kim, C. J.; Kim, Z. H.; Jo, M. H. *Appl. Phys. Lett.* **2008,** 92, 263111.
[28] Kim, C. J.; Lee, H. S.; Yang, Y. J.; Lee, R. R.; Lee, J. K.; Jo, M. H. *Adv. Mater.* **2011,** 23, 1025.
[29] Kanungo, P. D.; Wolfsteller, A.; Zakharov, N. D.; Werner, P.; Gosele, U. *Microe-letronics Journal* **2009,** 40, 452.
[30] Zakharov, N. D.; Werner, P.; Gerth, G.; Schubert, L.; Sokolov, L.; Gosele, U. *Journal of Crystal Growth.* **2006,** 290, 6.
[31] Sirbuly, D. J.; Law, M.; Pauzauskie, P.; Yan, H.; Maslov, A. V.; Knutzen, K.; Ning, C. Z.; Saykally, R. J.; Yang, P. D. *Proc. Nat. Acad. Sci. USA* **2005,** 102, 7800.
[32] Dong, A.; Wang, F.; Daulton, T. L.; Buhro, W. E. *Nano Lett.* **2007,** 7, 1308.
[33] Kim, C. J.; Kang, K.; Woo, Y. S.; Ryu, K. G.; Moon, H.; Kim, J. M.; Zang, D. S.; Jo, M. H.; *Adv. Mater.* **2007,** 19, 3637.
[34] Pan, A. L.; Liu, R. B.; Sun, M. H.; Ning, C. Z. *J. Am. Chem. Soc.* **2009,** 131, 9502.
[35] Liu, Y.; Zapien, J. A.; Shan, Y. Y.; Geng, C. Y.; Lee, C. S.; Lee, S. T. *Adv. Mater.* **2005,** 17, 1372.
[36] Pan, A. P.; Zhou, W. C.; Leong, E. S. P.; Liu, R. B.; Chin, A. H.; Zhou, B. S.; Ning, C. Z. *Nano. Lett.* **2009,** 9, 784.
[37] Kuykendall, T.; Ulrich, P.; Aloni, S.; Yang, P. D. *Nat. Materials* **2007,** 6, 951.
[38] Pan, A. L.; Liu, R. B.; Sun, M. H.; Ning, C. Z. *ACS Nano* **2010,** 4, 671.
[39] Lee, J. Y.; Kim, D. S.; Park, J. *Chem. Mater.* **2007**, 19, 4663.

[40] Ding, Y.; Yang, Q.; Guo, X.; Wang, S. S.; Gu, F. X.; Fu, J.; Wan, Q.; Chen, J. P.; Tong, L. M. *Opt. Exp.* **2009,** 17, 21813.

SUPPORTING INFORMATION:

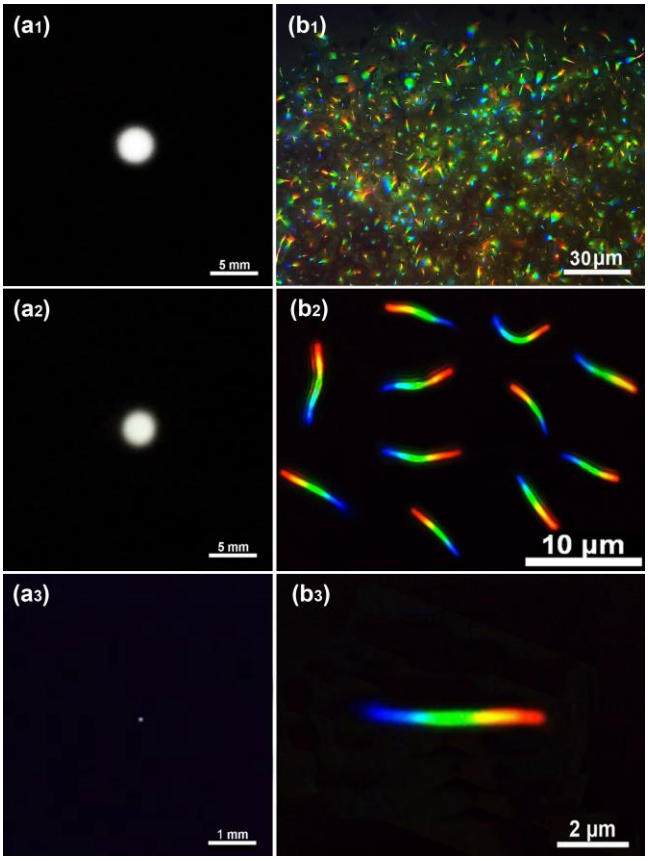

Figure S1

As shown in figure S1 ($a_{1\text{-}3}$), white light is generated when the size of nanowire comes to the resolution limit of the CCD/human eyes. Figure S1($b_{1\text{-}3}$) show the according products in three forms with the illuminations of 355 nm laser.

Table S1

Types of Tri-color Nanowire Samples	**Stay Time at P_1 (min)**	**$V_{P1\text{-}P2}$ (cm/min)**	**Stay Time at P_2 (min)**	**$V_{P2\text{-}P3}$ cm/min**	**Stay Time at P_3 (min)**
T_1(Short Red)	**6**	**15**	**4**	**15**	**1**
T_2(Long Red)	**4**	**15**	**4**	**15**	**5**
T_3(Short Blue)	**2**	**15**	**5**	**15**	**4**
T_4 (Pure White)	**5**	**15**	**4**	**15**	**3**

Notes: $V_{P1\text{-}P2}$ /$V_{P2\text{-}P3}$ (substrate moving speed in between positions P_1 and P_2/ P_2 and P_3) is conditioned by length of furnace cooling zoon.

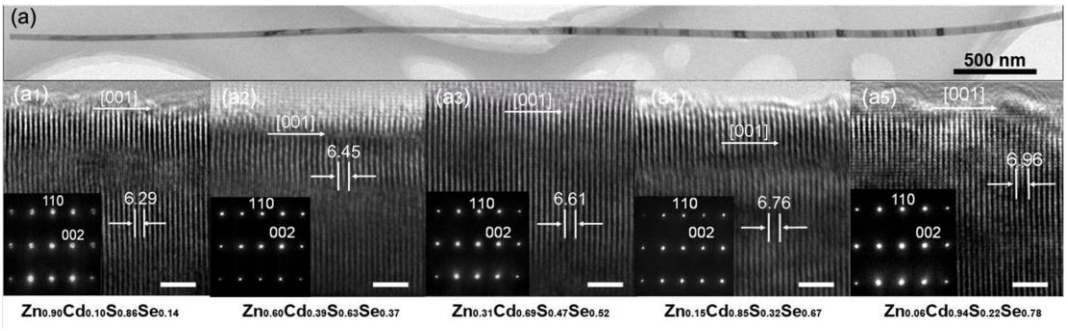

Figure S2

(a) TEM image of a typical RNW. (a_1-a_5) Corresponding HRTEM images and SAED patterns (Scale bar: 2 nm) taken from several representative regions along the length of the RNW shown in (a),

Figure S2 (a_1-a_5) are the HRTEM and SAED patterns taken from several representative regions along the length of the nanowire shown in figure S2 (a), and the alloy compositions for each region are shown below the respective images. The HRTEM and SAED patterns demonstrate that the nanowire is a single crystal with wurtzite structure.